

Investigation on the propagation mechanism of explosion stress wave in underground mining

Jiachen Wang^{1,2}, Fei Liu^{*1,2} and Jinwang Zhang^{**1,2}

¹College of Resources & Safety Engineering, China University of Mining & Technology, Beijing 100083, China

²Top-coal Caving Mining Research of Coal Mining Industry, Beijing 100083, China

(Received January 21, 2019, Revised February 12, 2019, Accepted February 19, 2019)

Abstract. The bedding plane has a significant influence on the effect of blasting fragmentation and the overall performance of underground mining. This paper explores the effects of fragmentation of the bedding plane and different angles by using the numerical analysis. ANSYS/LS-DYNA code was used for the implementation of the models. The models include a dynamic compressive and tensile failure which is applied to simulate the fractures generated by the explosion. Firstly, the cracks propagation with the non-bedding plane in the coal with two boreholes detonated simultaneously is calculated and the particle velocity and maximum principal stress at different points from the borehole are also discussed. Secondly, different delay times between the two boreholes are calculated to explore its effects on the propagation of the fractures. The results indicate that the coal around the right borehole is broken more fully and the range of the cracks propagation expanded with the delay time increases. The peak particle velocity decreases first and then increases with the distance from the right borehole increasing. Thirdly, different angles between the bedding plane and the centerline of the two boreholes and the transmission coefficient of stress wave at a bedding plane are considered. The results indicated that with the angles increase, the number of the fractures decreases while the transmission coefficient increases.

Keywords: underground mining; geological discontinuity; explosion-induced stress wave; fractures

1. Introduction

The traditional open pit mining cannot be used due to some of the coal mines are deeply buried. The most popular caving method for the mining of thick coal seam is an underground coal caving, the top-coal caving mining method (Wang *et al.* 2017, Yasitli *et al.* 2005, Wang *et al.* 2013, Li *et al.* 2009). However, the top coal cannot be broken fully during top coal mining when it comes to steeply inclined ultra-thick coal seams as Wudong mine in Western of China (Wang *et al.* 2014, Zhang *et al.* 2018). The geological structure of the mine was shown as follow.

As shown in Fig. 1, the coal seams have great dip degrees from about 45° to 90° and a thick of more than 20m. For the steeply inclined ultra-thick coal seams like this mine, the pre-blasting technique is usually used to solve the problems of top-coal inadequate destruction and large amounts of gas emission (Liu *et al.* 2015, Wang *et al.* 2000). Having a pre-fractured coal-rock mass around the caving zone will decrease the difficulty of the top coal caving and will avoid stress concentrations that can be dangerous if combined with the brittle behavior of the coal. One option to provide a pre-fractured coal zone to the caved zone is the use of explosives. That is, the auxiliary tunnel is

arranged in the coal to implement the weakening and crushing control technology for the top coal, so that the top coal can be smoothly discharged, and then the top coal mining technology can be used successfully. The schematic diagram of the sublevel top-coal caving mining method is shown in Fig. 2.

As shown in Fig. 2, the coal seam was divided into two horizontal sections. Two auxiliary tunnels and the boreholes were drilled in the coal from the auxiliary tunnels. The top coal was broken for a smoothly caving after the explosives were detonated.

The detonation of explosives in boreholes will cause dynamic stress wave propagation and quasi-static gas dilation under high temperature and pressure conditions (Yu *et al.* 2017, Han *et al.* 2016, Kalantari. 2011). The stress waves stimulate the original cracks in rock mass firstly, and then the explosion gas promotes the cracks propagation (Jeon 2015). The pre-existing cracks will arrest the propagation of radial cracks prematurely and the crack tips will lead to a further expansion of cracks in the rock (Hagan *et al.* 1977). There are also many pre-existing bedding planes in the coal which will affect the propagation of cracks during the pre-splitting blasting in underground coal caving. The coal explosion effect will be affected by the two holes blasting at the same time or with a delay time (Yang *et al.* 2012). However, the mechanism of stress wave propagation of two boreholes blasting with bedding planes is not very clearly understood.

It is hard to create the same experimental environment as the actual situation for the internal structure of coal and its rock stress cannot be re-established in the laboratory

*Corresponding author, Ph.D.

E-mail: feiliu182@163.com

**Corresponding author, Ph.D.

E-mail: jinwangzhang@hotmail.com

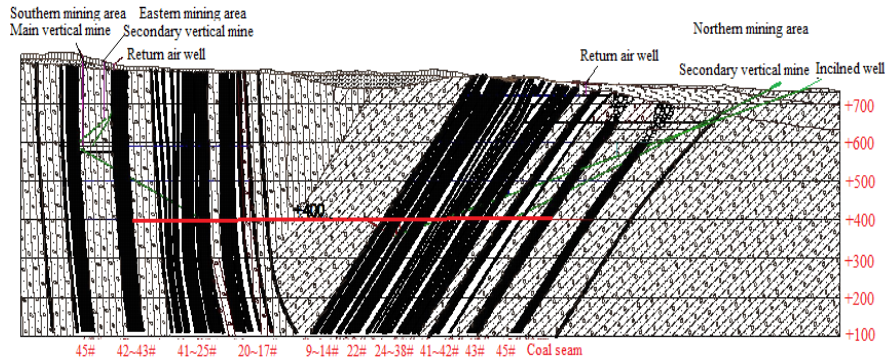


Fig. 1 Geological structure of Wudong mine

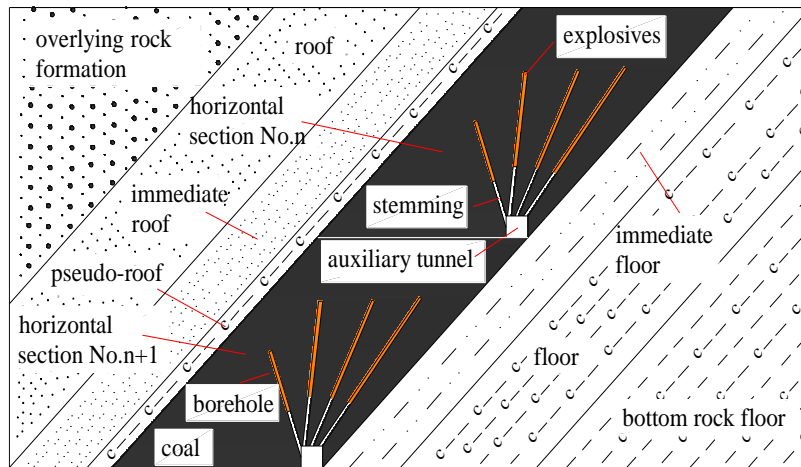


Fig. 2 Sublevel top-coal caving mining

environment. Numerical simulation as an important method can be used for this study (Zhang *et al.* 2018, Barla *et al.* 2012). Finite element models (FEMs) can be used as a blasting model to study the coal damage mechanism (Zhu *et al.* 2013). FEMs mainly use a continuum damage approach to describe the rock mass fractures during the blasting process and some researchers divide the blasting process into two phases: the fracture generation phase with shock waves, and the fracture growth phase with elastic waves (Zhao *et al.* 2017, Donze *et al.* 1997, Paine *et al.* 1994, Xie *et al.* 2016).

This paper explores the effects of simultaneously and different delay times of the two boreholes with a bedding plane to pre-fracture the coal. The bedding plane has different angles with the centerline of the two boreholes. The models compare the different fracture patterns and the explosion results generated at different scenarios as above. The detailed modeling process and the analysis of results are included as follows.

2. Numerical model implementation

2.1 General considerations

The numerical model consists of explosives, air and coal. Due to the considerable dimensions of the mining opening compared to the diameter of the borehole and the

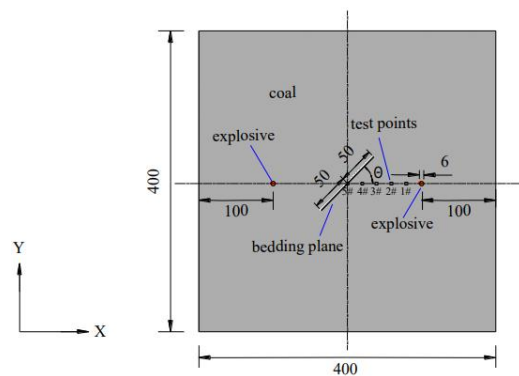


Fig. 3 Numerical model dimensions in centimeters

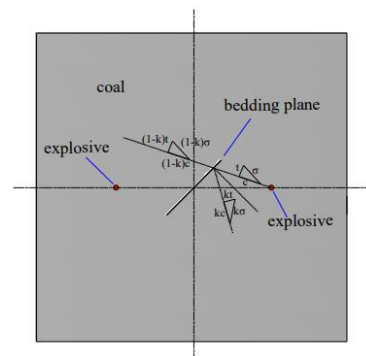


Fig. 4 Transmission and reflection waves at the bedding plane

thickness of the coal, the model was simplified into a plane strain conditions problem. In order to simulate an infinite boundary, the ideal condition is to create a larger size model so that it may not be affected by the stress wave reflection. However, a large model requires a high computer performance and a long calculate time which is not practical. LS-DYNA provides the non-reflection boundary conditions which can absorb the longitudinal (P) and shear (S) waves to eliminate the influence of reflecting stress waves at boundaries (LSTC 2003). The non-reflection boundary conditions are set at the boundaries of the models so the size of the model can be reduced.

Fig. 3 shows the geometry of the numerical models used in this paper. The coordinate system adopted is also shown in Fig. 3.

The total length of the bedding plane was 100 cm and the width was 0.8 cm. The center point of the bedding plane coincides with the center point of the model. The angle between the bedding plane and the centerline of the two boreholes is θ , which will be changed as 0° , 30° , 45° , 60° and 90° in different scenarios. Due to the gas was mixed composition, the material properties were not sure and that was not important to the crack propagation, the air was used as crack material when modeling. In order to investigate the stress propagation and crack expansion between the two boreholes, the points at the distance of 0.2 m, 0.4 m, 0.6 m, 0.8 m and 1.0 m from the right borehole as shown in Fig. 3 were set.

As shown in Fig. 4, when the stress waves induced by explosive detonation propagate to the bedding plane, the stress waves are divided into two parts: reflection waves and transmission waves (Zhao *et al.* 2017). Due to the bedding plane was filled with air, the transmission waves will be reduced a large part when crossing the bedding plane. The reflection waves will be changed to be a tensile wave and produced the spalling effect in the coal when propagated to the surface of the bedding plane. The proportion of these two parts is related to the angle between the bedding plane and the centerline of the two boreholes.

The software used was ANSYS/LS-DYNA. This software is a well-known generic finite element software that can be used to analyze the nonlinear dynamic response of a structure. Using the Arbitrary Lagrangian-Eulerian (ALE) finite element analysis method, explosives and air can be defined as a fluid and surrounding materials can be established as Lagrange units (Courtney L *et al.* 2016, An J *et al.* 2011). Fluid-structure coupling is used to make connections between the two materials so that substances can flow in the grid avoiding severe structural distortions of the elements. In this paper, the fluid-solid coupling algorithm is used to calculate the explosion effect of explosive on coal and the resultant crack propagation and distributions are analyzed. To facilitate modeling, a single-layer solid grid model was used with a non-reflected boundary at the around of the model and the thickness of the model is 1 centimeter.

2.2 Material properties in the model

2.2.1 Explosives

Kury and Lee (Kury *et al.* 1965, Lee *et al.* 1968) had

Table 1 Material parameters of Titan-6000-E1 Emulsion (Sanchidrian *et al.* 2015)

Density/ ρ_0 (Kg·m ⁻³)	Detonation speed /D (m·s ⁻¹)	CJ Pressure/ P_{CJ} (GPa)	CJ Relative volume/ V_{CJ}	Ideal explosion heat/Q (KJ/Kg)
890	4688	374	7.33	4.15

Table 2 JWL state parameters of Titan-6000-E1 Emulsion (Sanchidrian *et al.* 2015)

A(GPa)	B(GPa)	C(GPa)	R ₁	R ₂	ω	E ₀ (GPa)
209.685	3.509	0.517	5.762	1.290	0.39	2.386

done the accelerated metal experiments and got the detonation velocity and pressure of various explosives. The adiabatic expansion equation of detonation products is described by pressure, volume and energy (PVE) (Shi *et al.* 2005, Bai 2005). The Jones-Wilkens-Lee (JWL) equation of state was given by relating the pressure and specific volume generated in the detonation process which had been widely used in blasting calculations. It can be written as follows.

$$P = A \left(1 - \frac{\omega}{R_1 V} \right) e^{-R_1 V} + B \left(1 - \frac{\omega}{R_2 V} \right) e^{-R_2 V} + \frac{\omega E_0}{V} \quad (1)$$

In Eq. (1), A and B are parameters characteristic of the material, in GPa. The variables R₁, R₂, and ω are also parameters of the material. And P is pressure in, MPa, V is the relative volume, in m³, and E₀ is the initial specific internal energy, MJ.

The emulsion was used as the type of explosive material in the paper for the numerical models. Sanchidrian (Sanchidrian *et al.* 2015) tested a variety of emulsions and ANFO explosives by using the method of copper column expansion measurements and obtained the specific JWL state parameters of the explosives. The Titan-6000-E1 emulsion was used as the high-energy explosive in this paper. The parameters of the explosive shown in Table 1 and Table 2 are cited from the test results of Sanchidrian (Sanchidrian *et al.* 2015).

2.2.2 Coal

Coal has the similar mechanical properties as rock. Many numerical simulations on the mechanism of an explosion in rocks have been performed (Li *et al.* 2014, Ganesh *et al.* 2015, Vanessa *et al.* 2016, Timo 2010, Yu 2004). Hao (Hao *et al.* 2002) simulated the stress wave propagation and damage zone in the rock mass by programming and linking an anisotropic continuum damage model in Autodyn3D. Wang (Wang *et al.* 2007) analyzed dynamic fracture behavior of rock in tension due to blast loading by implementing the Taylor-Chen-Kuszmaul (TCK) continuum damage model together with an erosion algorithm into the explicit FE code of LS-DYNA.

However, few researchers show the propagation of the blasting wave and damage zone in coal. Wang (Wang *et al.* 1995) studied the basic dynamic behavior of the propagation of the explosion stress wave, explosion energy conversion, and explosion cavity expansion of columnar explosive for hard coal by using the experimental method of

Table 3 Material parameters of coal

Density/ ρ_0 ($Kg \cdot m^{-3}$)	Elastic modulus E (MPa)	Poisson's ratio	Yield stress (KN)	Tangent modulus (MPa)	Hardening coefficient	Failure strain
1860	2610	0.3	1.0	2.61	0.5	0.8

Table 4 The air material parameters (Bai 2005)

Density/ ρ ($g \cdot cm^{-3}$)	Dynamic viscosity coefficient/ μ	C_0	C_1	C_2	C_3	C_4	C_5	C_6	ν	E	Initial relative volume/ V_0
$1.18e^{-3}$	$1.75e^{-5}$	0	0	0	0	0.4	0.4	0	1.4	$2.5e^{-6}$	1

super dynamic strain and flash X-ray photographing on the large coal sample. The finite element numerical calculation method was used to simulate and analyze the effect of the pre-explosion of top coal.

By using some of the findings of previously mentioned researchers in coal, the numerical models in ANSYS/LS-DYNA are implemented in this paper. By following the procedures of the LS-DYNA keyword user's manual, the material properties of coal were implemented in the model (Paine *et al.* 1994).

The constitutive behavior selected for coal was a type of Plastic-Kinematic, which is suited to model kinematic hardening plasticity with the option of including strain-rate effects. The parameters for the coal material was based on the type and the in site coal of Jiangcang mine in western of China was included in Table 3 (Zhao *et al.* 2017, Bai 2005).

In Table 3, $A_0 \sim A_2$ are yield function constant for plastic yield function, $EPS_1 \sim EPS_{10}$ are volumetric strain values (natural logarithmic values), and $P_1 \sim P_{10}$ are pressures corresponding to volumetric strain values, in KN.

2.2.3 Air

The air material has no yield strength and behaves in a fluid-like manner by using the keyword MAT_NULL which was modeled with no shear stiffness and small hourglass coefficient to prevent energy losses. A (deviatoric) viscous stress of the form $\sigma_{ij} = \mu \dot{\epsilon}_{ij}$ is computed for nonzero μ where $\dot{\epsilon}_{ij}$ is the deviatoric strain rate, μ is the dynamic viscosity with a unit of [Pascal*second]. The equation of state of air can be described by keyword LINEAR_POLYNOMIAL as follows.

$$P = (C_0 + C_1 v + C_2 v^2 + C_3 v^3) + (C_4 + C_5 v + C_6 v^2) E \quad (2)$$

where $C_0 \sim C_6$ are coefficients of the equation; v is specific volume, which is 1.4 for air; E is specific energy. The parameters for the air material is included in Table 4 (Bai 2005).

2.3 Meshing results

Two boreholes with a circle of radius 3 cm were created in the three-dimensional single-layer solid grid model. The meshing method for the explosives and bedding plane was mapping with quadrilateral. While the meshing method for the coal mass was sweeping with quadrilateral due to the angle between the bedding plane and the centerline of the two boreholes was changed. So it is better to be meshed by

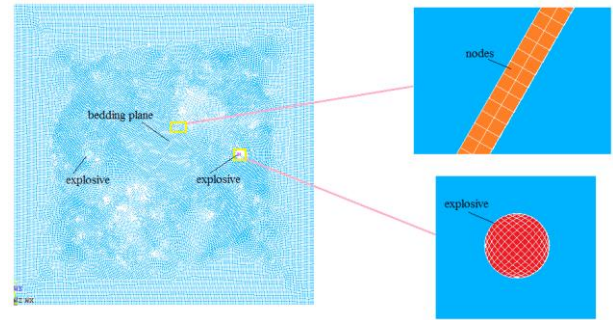


Fig. 5 Meshing results with bedding plane and explosives at 60°

sweeping for the coal mass. The meshing results for explosives, bedding plane and coal mass were shown in Fig. 5 when the angle between the bedding plane and the centerline of the two boreholes was 60°.

As shown in Fig. 5, the bedding plane and the explosives were meshed by mapped and the coal mass was meshed by the sweep method. The numbers of the explosives, bedding plane and the coal mass elements used in the simulation are 142, 500 and 42587, respectively at 60° of the angle between the bedding plane and the centerline of the two boreholes.

In the initial part of the research, a model with a non-bedding plane in Fig. 6 was implemented to investigate the propagation of cracks in the model. Then a bedding plane with different angles with the centerline of the two boreholes was simulated.

3. Structural reliability analysis

3.1 Results with no bedding plane

Fig. 6 includes the results of the stress contours with no bedding plane between the two boreholes. The explosion process was shown at 299 μ s, 1050 μ s, 1450 μ s and 2700 μ s after the explosion, respectively. In order to have a clear display, the explosives and air material were hidden during the explosion process.

Fig. 6(a) shows that after 299 μ s, the explosion stress waves have been formed and spread out from the two boreholes. The high-stress zone formed a circle in front of the stress waves. As shown in Fig. 6(a), compression cracks appeared around the borehole in the zone of the explosive. It was mainly because the stress wave generated by the explosion impacting the wall of the borehole and reaching the dynamic compressive strength of the coal, starting the initial crushing zone around the borehole. The high-temperature and high-pressure gas generated by the explosion then enters the fractures, forming a stress concentration at the tip of the fracture, allowing the fracture to continue to expand forward. Some cracks appeared in the coal after the explosion stress wave passed. At some areas of the model, the stress wave does not break the coal because its amplitude is lower than the compressive strength of the coal. During the transmission process of the stress wave, an accumulation of elastic potential energy in the coal was observed. After the stress wave had passed, the

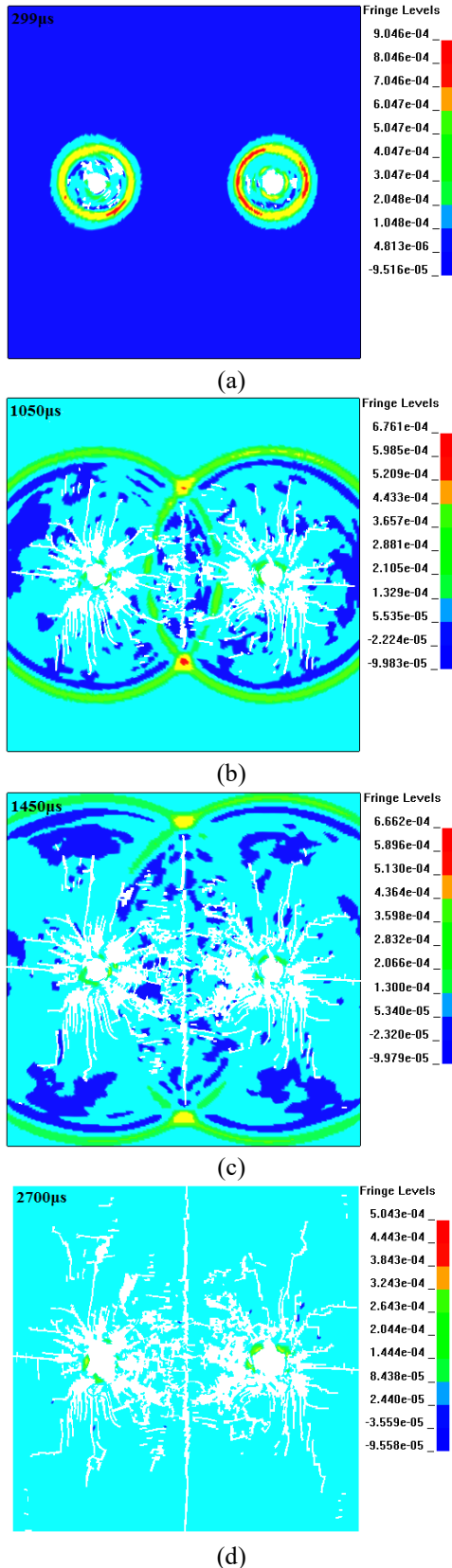


Fig. 6 Explosion contours of stress obtained with no bedding plane

elastic potential energy is released quickly, generating tension in the coal and producing more fractures.

After 1050µs as shown in Fig. 6(b), the two stress waves

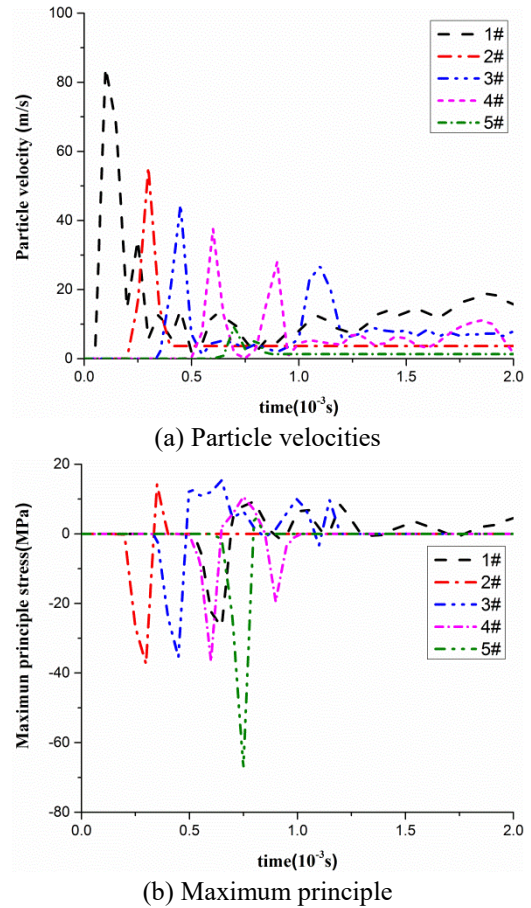


Fig. 7 Particle velocity and maximum principle stress with time

contact and interpenetrate each other. Compression and tensile cracks formed around the boreholes. Two high-stress points appeared at the overlapping areas of the stress waves and a vertical crack formed between the two points. As shown in Fig. 6(c) at 1450µs, more cracks formed in the penetration area of stress wave. It was due to many tiny cracks were produced in the coal far away from the boreholes for the first stress wave, and then the other stress wave came and induced the origin damage for a second broken. The explosion process is completed at 2700µs. The coal is broken fully with many cracks around the boreholes and a vertical crack appeared in the middle of the two boreholes. The density of cracks between two boreholes is larger than other areas due to the second broken of the stress wave.

Since explosion stress waves mainly induce particle movement in the coal, the particle velocity is used to describe the stress waves and the cracks propagation between the two boreholes after the explosion. The particle velocities at different points as shown in Fig. 2 were shown in Fig. 7(a). According to the first strength theory, the main factor of material damage is the maximum tensile stress which can be expressed by the maximum principle stress. Fig. 7(b) shows the maximum principle stress with time at a different distance from the right borehole.

As shown in Fig. 7(a), the peak of particle velocity reducing with the distance from the right borehole

increasing. It is due to the stress wave induced by the explosion attenuated in the coal with the distance from the borehole increasing. The peak of particle velocity at point 1# was 82 m/s which was much greater than that at point 2#. It was because the point 1# was very close to the borehole. Two obviously crests were formed and approaching each other with the distance increases. The peak of particle velocity at the point 5#, which is at the midpoint of the centerline of the two boreholes, was about 8 m/s. It is due to the two boreholes counterbalanced each other at that point.

Fig. 7(b) shows the maximum principle stress which can convey the crushing of coal at these points. As shown in the figure, the peaks of the maximum principle stress were almost the same (about -35 MPa) at the point of 2#, 3# and 4#. Due to the coal at point 1# is too close to the borehole, the peak of the maximum principle stress is lower (about -25 MPa) than others at that point. However, the peak of the maximum principle stress is the biggest (about 68 MPa) at point 5# for the coal at that point are affected by the explosion stress waves induced by the two explosives at the same time, which can result in the greatest broken effect.

3.2 Results with a delay time of 0.5 ms and 1.0 ms

The delay time of the two boreholes is also an important factor for the crushing of the coal between the two boreholes. A delay time of 0.5 ms and 1.0 ms are installed in the model by the left explosive detonated first and then the right explosive detonated to test the crushing effects with different angles. The crushing processes with a delay time of 0.5 ms and 1.0 ms are shown in Figs. 8 and 9.

As shown in Fig. 8(a), the left explosive detonated and propagated with many cracks around the borehole and some tiny cracks far away from the left borehole. And the right explosive started detonation. In Fig. 8(b), two high stress points appeared for the superposition of the two stress waves when the first stress wave spread to the right borehole. As shown in Fig. 8(c), many cracks formed in the overlapping area of the two stress waves. It is due to the coal has been damaged and formed many tiny cracks by the first stress wave. Then the right explosive detonated and formed an explosion stress wave which has a second broken on the damaged coal and excited the tiny cracks propagation. An arc crack zone formed following the two high stress points for the superposition of the two stress waves. Fig. 8(d) shows the final crushing effect with the delay time of 0.5 ms. Many cracks formed around the two boreholes and some cracks also appeared between the two boreholes. Many new tiny cracks were formed on the cracks induced by the left explosive due to the second broken of the right explosive.

As shown in Fig. 9(a), the left explosive detonated and the stress wave propagated with many cracks formed around the left borehole. Some ring cracks formed around the right borehole as the explosion stress wave propagated to the right borehole. In Fig. 9(b), the right explosive starts to detonate. Meantime, the stress wave induced by the left explosive has spread over from the right borehole. In Fig. 9(c), high-density cracks were formed around the right borehole due to the second broken of the explosion stress

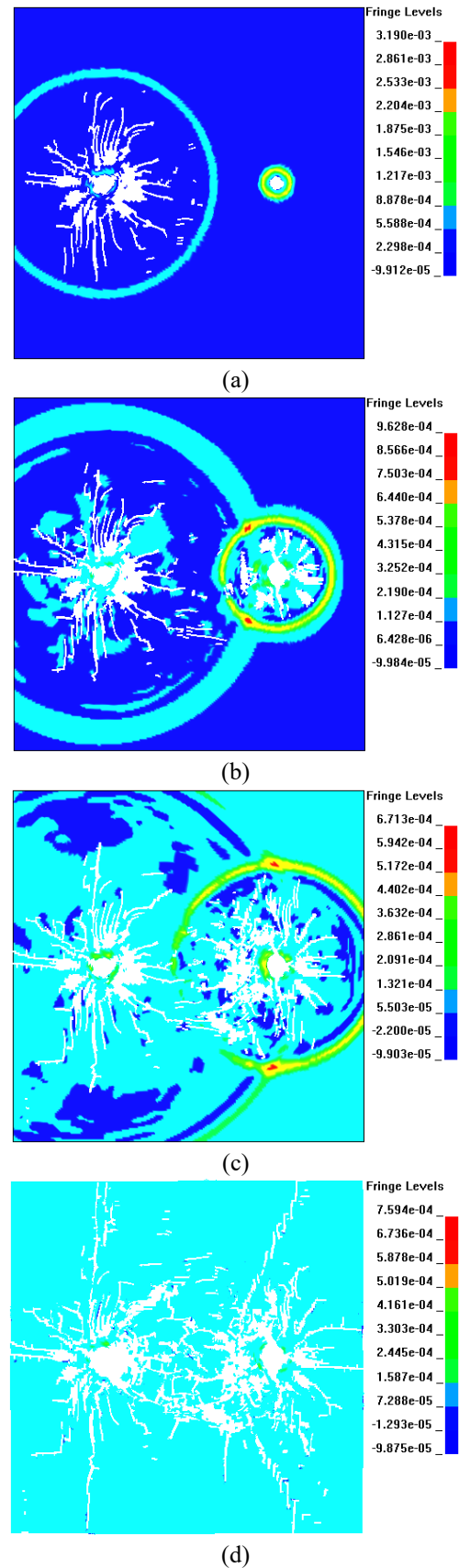


Fig. 8 Crushing process with a delay time of 0.5 ms

wave induced by the right explosive. The first stress wave propagated followed by the second stress wave which

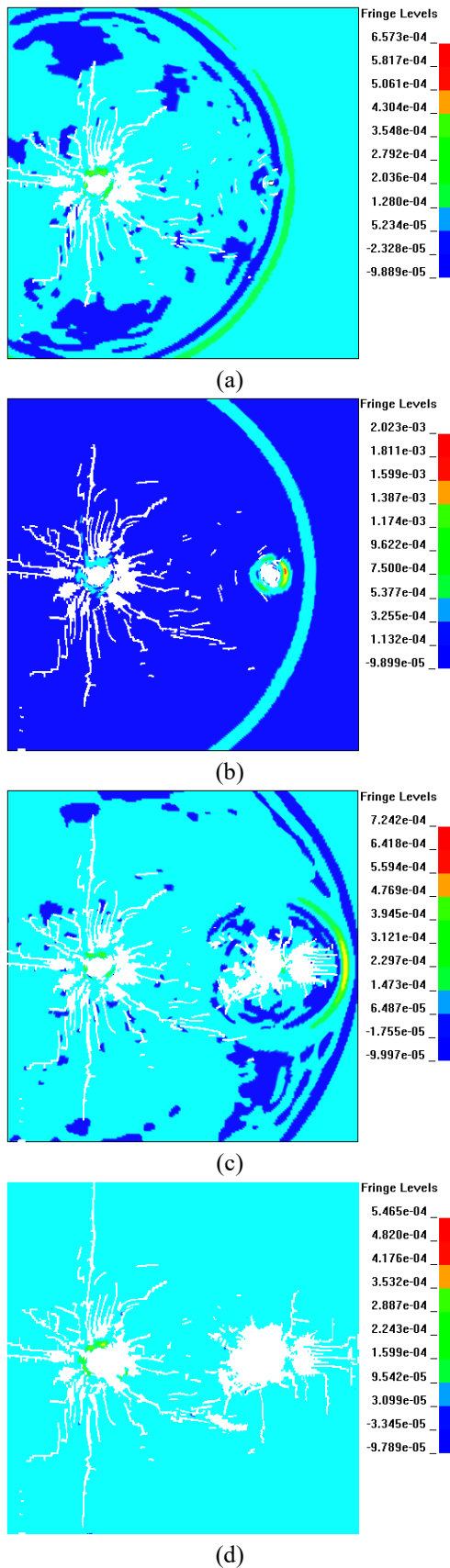


Fig. 9 Crushing process with a delay time of 1.0 ms

cannot catch up it. An arc-shaped high-stress wave was formed in the second stress wave near to the first stress

wave. Fig. 9(d) shows the final crushing effect with the delay time of 1.0ms. The cracks around the left borehole were propagated dispersed and far away. However, the cracks around the right borehole were more concentrated around the borehole with few cracks far away and few cracks between the two boreholes. Some horizontal cracks were formed at the right lateral of the right borehole due to the tensile of the arc-shaped high-stress wave.

3.3 Other scenarios results

The bedding plane with a different angle with the centerline of the two boreholes was added in the center point of the model. The main purpose of the scenarios is to investigate the explosion stress waves and the cracks propagation across the bedding plane. For the first stress wave generated by the left explosive has spread over the right borehole with the delay time of 1.0 ms, the delay time has been considered to 1.0 ms due to a longer delay time will have a minor different crushing effect in the coal. The final crushing effects for the scenarios are included in Fig. 10 for three conditions: a) Two boreholes are detonated simultaneously; b) The left explosive is detonated first while the right explosive is detonated with a delay time of 0.5 ms and c) The delay time of the right explosive is 1.0 ms.

As seen in Fig. 10, there is evidence of more cracks between the two boreholes when a bedding plane is added in the center of the model compared with the non-bedding plane. And a significant change of the cracks propagation was observed with the delay time increases. As shown in Fig. 10, the vertical crack between the two boreholes spread near to the right borehole and presenting an arc for the stress waves overlay each other at a delay time of 0.5 ms. And the number of the cracks between the two boreholes seems to decrease when compared with the delay time of 0 ms. At the delay time of 1.0 ms, the vertical crack dispersed for the two stress waves have no stress overlapping. The number of cracks between the two boreholes at a delay time of 1.0 ms is less than that of the two delay time before. The coal around the right borehole was broken fully for the second broken of the stress wave induced by the right explosive.

At the scenario with the angle of 0° between the bedding plane and the centerline of the two boreholes, the coal between the two boreholes has more cracks with a delay time of 0 ms and 0.5 ms compared with the non-bedding plane. And the cracks more concentrated around the boreholes. There are more fractures between the two boreholes and around the right borehole at the delay time of 1.0 ms compared with the non-bedding plane. It is due to the stress wave will be reflected when encountered with the bedding plane and changed as a tensile wave, which is the main factor to broken the coal.

The coal will produce the spalling effect at the surface of the bedding plane when the angle changed from 30° to 90° . And the cracks between the two boreholes will be changed with angle changing. As shown in Fig. 10, the number of the fractures will decrease the same delay time with the angle increasing. It is due to the propagation of stress wave will be blocked when it encountered the

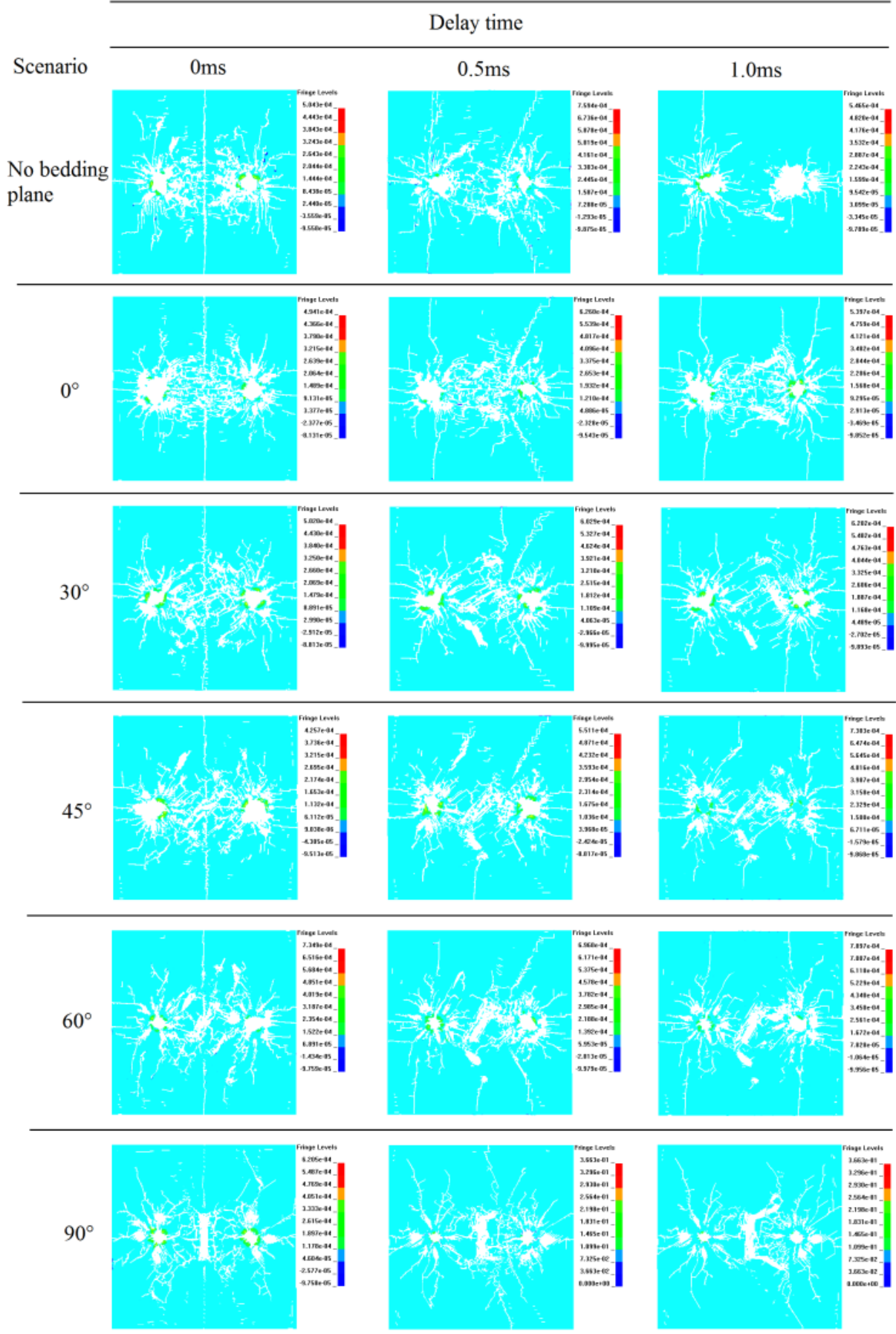


Fig.10 Final crushing effects for different scenarios

bedding plane. With the angle increases, more stress waves will be blocked. Therefore, the function of the block is more significant. With the delay time increases, the range of the cracks propagation also expanded. It is because the coal mass was damaged by the first stress wave induced by the left explosive, then the second stress wave induced by the right explosive will have a second broken on the damage zone. So, the coal far away from the borehole will also be broken for the second stress wave induced by the right explosive.

As mentioned before, the particle velocity was used to describe the propagation of stress waves between the two boreholes after the explosion. The peak particle velocity of the points away from the right borehole with a distance of 0.2 m, 0.4 m, 0.6 m, 0.8 m and 1.0 m at different angles were calculated. The results were shown in Fig. 11(a)-11(c) with a delay time of 0 ms, 0.5 ms and 1.0 ms, respectively.

As shown in Fig. 11(a), the peak particle velocity showed a trend of decreasing with the distance from the right borehole increasing at the delay time of 0 ms. However, the peak particle velocity increased at the distance of 1.0 m from the right borehole (the midpoint of the two boreholes) at the angle of 30°, 45° and 60°. It is because the propagation of the stress waves was changed for the bedding plane and has a concentrated effect for the overlying on the midpoint. The peak particle velocity continues decreasing at the distance of 1.0 m from the right borehole. The peak particle velocity is the lowest (about 8 m/s) at the midpoint between the two boreholes at the scenario of no bedding plane. It is because the two explosives are detonated at the same time and the stress waves are not changed by the bedding plane and spread to the midpoint also at the same time. The particle at that point has a low peak velocity for the stress waves are counteracted by each other.

In Fig. 11(b), all curves have a similar trend of the peak particle velocity decreasing first and then increasing with the distance from the right borehole increasing at the delay time of 0.5 ms. It is due to the left explosive are detonated first and the stress wave spread with cracks propagated over the midpoint. Then the right explosive detonated and stress wave propagated. Due to the cracks induced by the left explosive, the propagation of the stress wave induced by the right explosive was obstructed and has a lower effect on the midpoint than the first stress wave induced by the left explosive. So the high values at the distance of 1.0 m from the right borehole are formed by the left explosive. The peak particle velocities at different scenarios have a similar value with a high coincidence degree and only a few velocities at the midpoint are dispersed. It is due to the coal at the midpoint are crushed by the stress wave and have a different effect on the peak particle velocity.

As shown in Fig. 11(c), the curves have a similar trend as the Fig. 11(b) with the peak particle velocity decreasing first and then increasing with the distance from the right borehole increasing at the delay time of 1.0 ms. However, the curves are more dispersed than that in Fig. 11(b) due to a longer delay time. The coal near the right borehole is crushed more fully with the delay time of 1.0 ms. As shown in Fig. 8, the first stress wave induced by the left explosive has spread over the right borehole when the right explosive

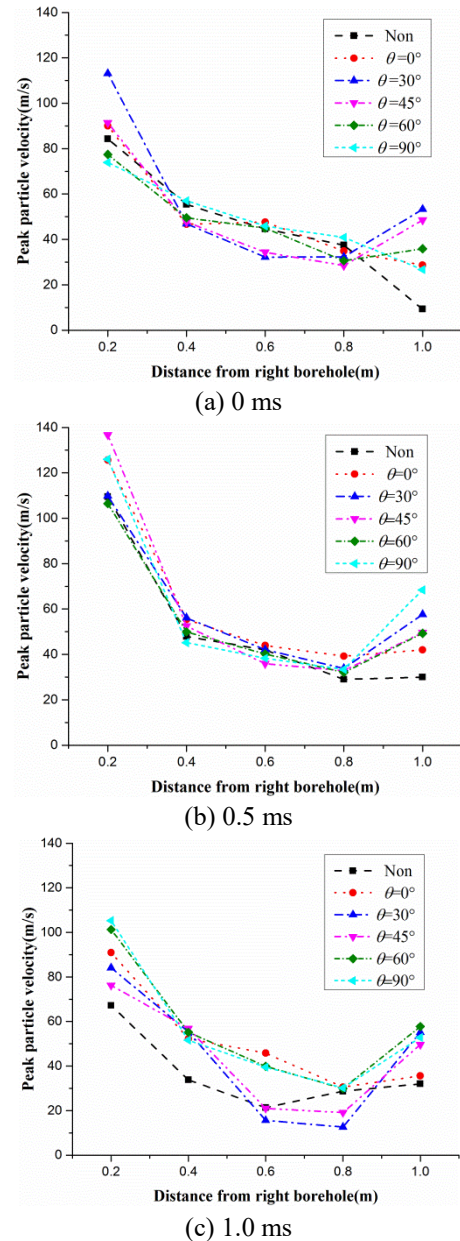


Fig. 11 Peak particle velocity at different delay time

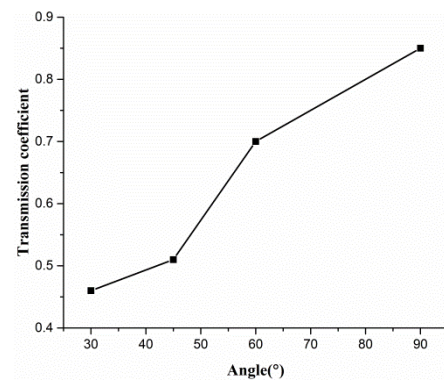


Fig. 12 Transmission coefficient with angle

start detonated. So the coal between the midpoint and the right borehole has broken and some cracks are formed. Then the stress waves induced by the right explosive start

propagated and the peak particle velocity dispersed for the effect of crushed coal.

The distributions of stress waves before and after the stress wave propagate across the bedding plane can be described by the peak particle velocity. The transmission coefficient (T_{coe}) of stress waves at a bedding plane can be expressed as $T_{coe} = V_{tra} / V_{inc}$ (Note that V_{inc} is incident peak particle velocity and V_{tra} is transmission peak particle velocity) (Zhao *et al.* 2001). As shown in Fig. 4, the stress wave will be reduced when crossing the bedding plane due to some of them is blocked and the other is reflected by the bedding plane. The transmission coefficient (T_{coe}) of the stress waves at the bedding plane in different scenarios is shown as bellow in Fig. 12. Due to the transmission coefficient will not be affected by the delay time with a single explosive, the transmission coefficients are tested at the delay time of 1.0 ms near the bedding plane.

The transmission coefficient of the single explosive at the bedding plane with different angles is shown in Fig. 12. Due to the bedding plane is horizontal at the angle of 0° and the explosion stress wave is propagated parallel through the bedding plane, the transmission coefficient is not considered at 0° in Fig. 12.

As shown in Fig. 12, the transmission coefficient of stress wave at bedding plane is increasing with the angles between the bedding plane and the centerline of the two boreholes increasing. The transmission coefficient is about 0.46 at the angle of 30° which means only 46% of the stress wave was penetrated through the bedding plane due to the blocked and the reflection of the bedding plane. With the angle increasing from 45° to 60° , the transmission coefficient has a large improve from 0.51 to 0.70. The stress wave propagates vertically through the bedding plane at the angle of 90° and has the highest transmission coefficient of 0.84, which have a clear indication that the boreholes should be arranged vertically with the bedding plane for the minimum reduction of the stress wave when crossing the bedding plane.

4. Conclusions

The explosion contours of stress and the fracture of the coal were obtained by using numerical calculation software ANSYS/LS-DYNA. The effects of bedding plane and the angle between the bedding plane and the centerline of the two boreholes on coal mass fracture patterns are investigated. The calculation results were post-processed to obtain particle velocities and maximum principle stress. The following conclusions can be obtained through comprehensive analysis.

The bedding plane has a significant influence on the cracks formation and propagation and can increase the number of cracks. The delay time between the left explosive detonation and the right explosive detonation has a significant influence on the cracks propagation. As the delay time increases, the cracks propagated tilt to the right borehole and the coal around the right borehole is broken more fully. The range of the cracks propagation expanded with the delay time increases.

Due to the reflection of stress wave at the bedding plane,

the fracture between the bedding plane and the borehole can be enhanced. With the angle increases, more stress waves will cross through the bedding plane and less reflection tensile waves are formed which is the main reason for the crushing of coal. The number of the fractures decreases with the angle increasing.

The peak particle velocity on the centerline of the two boreholes decreases first and then increases at the midpoint with the distance from the right borehole increasing. The transmission coefficient increases with the angle increasing. When the angle is 90° , the stress wave propagates vertically through the bedding plane and has the highest transmission coefficient of 0.84.

Acknowledgements

This research is supported by the National Natural Science Foundation of China (No.51674264, No.51574244) and National Key Research and Development Program of China (No.2017YFC0603002, No.2018YFC0604501).

References

- An, J., Tuan, C.Y. and Cheeseman, B.A. (2011), "Simulation of soil behavior under blast loading", *Int. J. Geomech.*, **11**(4), 323-334.
- Bai, J.Z. (2005), *Theoretical Basis and Case Analysis of LS-DYNA3D*, Science Press, Beijing, Beijing, China.
- Barla, M., Piovano, G. and Grasselli, G. (2012), "Rock slide simulation with the combined finite-discrete element method", *Int. J. Geomech.*, **12**(6), 711-721.
- Courtney, L., Catherine, T. and Rafiqul, A. (2016), "Experimental evaluation and finite-element simulations of explosive airblast tests on clay soils", *Int. J. Geomech.*, **16**(4), 04015097.
- Donze, F.V., Bouchez, J. and Magnier, S.A. (1997), "Modeling fractures in rock blasting", *Int. J. Rock Mech. Min. Sci.*, **34**(8), 1153-1163.
- Ganesh, T., Anirudha, V.K. and Stephen, R. (2015), "Experimental and finite element analysis of doubly reinforced concrete slabs subjected to blast loads", *Int. J. Impact Eng.*, **75**, 162-173.
- Hagan, T.N. (1977), "Rock breakage by explosives", *Proceedings of the 6th Colloquium on Gasdynamics of Explosions and Reactive Systems*, Stockholm, Sweden, August.
- Han, Y.Z. and Liu, H.B. (2016), "Failure of circular tunnel in saturated soil subjected to internal blast loading", *Geomech. Eng.*, **11**(3), 421-438.
- Hao, H., Wu, C. and Zhou, Y. (2002), "Numerical analysis of blast-induced stress waves in a rock mass with anisotropic continuum damage models part 1: Equivalent material property approach", *Rock Mech. Rock Eng.*, **35**(2), 79-94.
- Jeon, S., Kim, T.H. and You, K.H. (2015), "Characteristics of crater formation due to explosives blasting in rock mass", *Geomech. Eng.*, **9**(3), 329-344.
- Kalantari, B. (2011), "Strength evaluation of air cured, cement treated peat with blast furnace slag", *Geomech. Eng.*, **3**(3), 207-218.
- Kury, J.W., Lee, E.L. and Hornig, H.C. (1965), "Metal acceleration by chemical explosives", *Proceedings of the 4th Detonation Symposium*, White Oak, Maryland, U.S.A., October.
- Lee, E.L., Hornig, H.C. and Kury, J.W. (1968), *Adiabatic Expansion of High Explosive Detonation Products*, University of California, Livermore, California, U.S.A.
- Li, C.R., Kang, L.J. and Qi, Q.X. (2009), "The numerical analysis

- of borehole blasting and application in coal mine roof-weaken", *Proc. Earth Plan. Sci.*, **1**(1), 451-459.
- Li, J. and Hao, H. (2004), "Numerical study of concrete spall damage to blast loads", *Int. J. Impact Eng.*, **68**, 41-55.
- Liu, J., Liu, Z.G. and Xue, J. (2015), "Application of deep borehole blasting on fully mechanized hard top-coal pre-splitting and gas extraction in the special thick seam", *Int. J. Min. Sci. Technol.*, **25**(5), 755-760.
- Livermore Software Technology Corporation (LSTC). (2003), *LS-DYNA Keyword User's Manual*, Version 970, Livermore, California, U.S.A.
- Paine, A.S. and Please, C.P. (1994), "An improved model of fracture propagation by gas during rock blasting-Some analytical results", *Int. J. Rock Mech. Min. Sci. Geomech. Abstr.*, **31**(6), 699-706.
- Sanchidrian, J.A., Castedo, R. and Lopez, L.M. (2015), "Determination of the JWL constants for ANFO and emulsion explosives from cylinder test data", *Central Euro. J. Energ. Mater.*, **12**(2), 177-194.
- Shi, D.Y., Li, Y.C. and Zhang, S.M. (2005), *Display Dynamic Analysis Based on ANSYS/LS-DYNA8.1*, Tsinghua University Press, Beijing, China.
- Timo, S. (2010), "Damage-viscoplastic consistency model with a parabolic cap for rocks with brittle and ductile behavior under low-velocity impact loading", *Int. J. Numer. Anal. Meth. Geomech.*, **34**(13), 1362-1386.
- Vanessa, P., Huon, B. and Pat, M. (2016), "Analysis of the structural response and failure of containers subjected to internal blast loading", *Int. J. Impact Eng.*, **95**, 40-53.
- Wang, F.T., Tu, S.H. and Yuan, Y. (2013), "Deep-hole pre-split blasting mechanism and its application for controlled roof caving in shallow depth seams", *Int. J. Rock Mech. Min. Sci.*, **64**, 112-121.
- Wang, J.C. and Li, Y. (2017), *Thick Seam Coal Mining and its Ground Control*, in *Advances in Coal Mine Ground Control*, Woodhead Publishing, Cambridge, Sawston, U.K.
- Wang, J.C., Bai, X.J. and Wu, Z.S. (2000), "The research on the fractured blocks of the top-coal in the longwall top-coal caving technique of the hard coal seam", *J. China Coal Soc.*, **25**(3), 238-242.
- Wang, J.C., Yang, S.L. and Li, Y. (2014), "Caving mechanisms of loose top coal in longwall top coal caving mining method", *Int. J. Rock Mech. Min. Sci.*, **71**, 160-170.
- Wang, X.L. and Suo, Y.L. (1995), "Computer simulation of pre-explosion of fully mechanized coal caving roof in hard coal seam", *J. Xi'an Min. Inst.*, **15**, 97-101.
- Wang, Z.L., Li, Y.C. and Shen, R.F. (2007), "Numerical simulation of tensile damage and blast crater in brittle rock due to underground explosion", *Int. J. Rock Mech. Min. Sci.*, **44**(5), 730-738.
- Xie, L.X., Lu, W.B. and Zhang, Q.B. (2016), "Damage evolution mechanisms of rock in deep tunnels induced by cut blasting", *Tunn. Undergr. Sp. Technol.*, **58**, 257-270.
- Yang, R.S., Wang, Y.B. and Xue, H.J. (2012), "Dynamic behavior analysis of perforated crack propagation in two-hole blasting", *Proc. Earth Plan. Sci.*, **5**, 254-261.
- Yasitli, N.E. and Unver, B. (2005), "3D numerical modeling of longwall mining with top-coal caving", *Int. J. Rock Mech. Min. Sci.*, **42**(2), 219-235.
- Yu, A.B. (2004), "Discrete element method: An effective way for particle scale research of particulate matter", *Eng. Comput.*, **21**, 205-214.
- Yu, L.Y., Su, H.J. and Jing, H. (2017), "Experimental study of the mechanical behavior of sandstone affected by blasting", *Int. J. Rock Mech. Min. Sci.*, **93**, 234-241.
- Zhang, J.W., Wang, J.C. and Wei, W.J. (2018), "Experimental and numerical investigation on coal drawing from thick steep seam with longwall top coal caving mining", *Arab. J. Geosci.*, **11**(96), 1-19.
- Zhang, Y.T., Ding, X.L. and Huang, S.L. (2018), "Field measurement and numerical simulation of excavation damaged zone in a 2000 m-deep cavern", *Geomech. Eng.*, **16**(4), 399-413.
- Zhao, J. and Cai, J.G. (2001), "Transmission of elastic P-waves across single fractures with a non-linear normal deformational behavior", *Rock Mech. Rock Eng.*, **34**(1), 3-22.
- Zhao, J.J., Zhang, Y. and Ranjith, P.G. (2017), "Numerical simulation of blasting-induced fracture expansion in coal masses", *Int. J. Rock Mech. Min. Sci.*, **100**, 28-39.
- Zhu, W.C., Wei, C.H. and Li, S. (2013), "Numerical modeling on destress blasting in coal seam for enhancing gas drainage", *Int. J. Rock Mech. Min. Sci.*, **59**, 179-190.

CC